Threshold photoelectron photoion coincidence spectroscopy and selected ion flow tube cation-molecule reaction studies of cyclic-C4F8

Parkes, Michael A.; Ali, Sahangir; Tuckett, Richard P.; Mikhailov, Victor A.; Mayhew, Christopher

DOI:
10.1039/b604726b

Threshold photoelectron photoion coincidence spectroscopy and selected ion flow tube cation-molecule reaction studies of cyclic-C_4F_8†

Michael A. Parkes,[a] Sahangir Ali,[a] Richard P. Tuckett,*[a] Victor A. Mikhailov[b] and Chris A. Mayhew[b]

Received 3rd April 2006, Accepted 20th June 2006
First published as an Advance Article on the web 30th June 2006
DOI: 10.1039/b604726b

Using tunable vacuum-UV radiation from a synchrotron, the threshold photoelectron and threshold photoelectron photoion coincidence (TPEPICO) spectra of cyclic-C_4F_8 in the range 11–25 eV have been recorded. The parent ion is observed very weakly at threshold, 11.60 eV, and is most likely to have cyclic geometry. Ion yield curves and branching ratios have been determined for five fragments. Above threshold, the first ion observed is $C_3F_5^+$, at slightly higher energy $C_2F_4^+$, then successively CF^+, CF_2^+ and CF_3^+ are formed. The dominant ions are $C_3F_5^+$ and $C_2F_4^+$, with the data suggesting the presence of a barrier in the exit channel to production of $C_3F_5^+$ whilst no barrier to production of $C_2F_4^+$. In complementary experiments, the product branching ratios and rate coefficients have been measured in a selected ion flow tube (SIFT) at 298 K for the bimolecular reactions of cyclic-C_4F_8 with a large number of atomic and small molecular cations. Below the energy where charge transfer becomes energetically allowed, only one of the ions, CF_2^+, reacts. Above this energy, all but one of the remaining ions react. Experimental rate coefficients are consistently greater than the collisional values calculated from modified average dipole orientation theory. The inclusion of an additional ion–quadrupole interaction has allowed better agreement to be achieved. With the exception of N^+, a comparison of the fragment ion branching ratios from the TPEPICO and SIFT data suggest that long-range charge transfer is the dominate mechanism for reactions of ions with recombination energy between 12.9 and 15.8 eV. For all other ions, either short-range charge transfer or a chemical reaction, involving cleavage and making of new bond(s), is the dominant mechanism.

1. Introduction

Octafluorocyclobutane, given the abbreviation *c*-C_4F_8 throughout this paper, is an important industrial gas, especially in plasma processing.[1–3] It is used extensively in dry etching processes due to its high selectivity over other fluorocarbon feed gases,[1] and it is also used for high-voltage insulation, especially in *c*-C_4F_8/SF_6 mixtures. Here, the rapid rate coefficient for non-dissociative electron attachment to *c*-C_4F_8 makes it more suitable than other insulating mixtures.[4] Due to these advantages, there have been many studies on the interaction of electrons with *c*-C_4F_8.[4–7] There have also been studies of dissociation of *c*-C_4F_8 induced by infrared (IR) radiation[8] and by thermal decomposition.[9,10] Spectroscopic studies include gas-phase electron diffraction[11] and IR measurements.[12] The absence of a dipole moment means that *c*-C_4F_8 shows no microwave spectrum. The electronic spectra occur at higher energies than those corresponding to the visible/UV region, confirming the stability of this closed-shell molecule. Ravishankara *et al.*[13] report that the lifetime of this molecule in the earth's atmosphere is very long, *ca.* 1000 years, but this value is shorter than other long-lived perfluorocarbon molecules due to its significant absorption of Lyman-α radiation at 121.6 nm. The use of this gas in industry therefore has major atmospheric implications for global warming. At higher energies, there have only been three studies on the photoionisation or positive ion chemistry of *c*-C_4F_8.[14–16] The one measurement of any kind of photoelectron spectrum was reported by our group eight years ago,[17] and some chemical reactions of *c*-$C_4F_8^-$ were recently reported by Hiraoka *et al.*[18] The photoelectron spectrum was part of a study of the fragmentation of valence states of *c*-$C_4F_8^+$ by coincidence techniques, and used a 1 metre Seya vacuum-UV monochromator at the Daresbury Synchrotron Radiation Source (SRS), UK. We have now repeated these threshold photoelectron photoion coincidence (TPEPICO) measurements using a higher-flux monochromator at Daresbury. Furthermore, we have extended the ion-molecule study of Morris *et al.*,[16] and report the first comprehensive study of the kinetics and products of the reactions of *c*-C_4F_8 with a range of gas-phase cations using a selected ion flow tube (SIFT).

Both experiments give information on the products formed upon ionisation of a neutral precursor molecule. This information can give insight into whether each ion-molecule reaction proceeds *via* charge transfer, *i.e.* the hopping of an

[a] *School of Chemistry, University of Birmingham, Edgbaston, Birmingham, UK B15 2TT. E-mail: r.p.tuckett@bham.ac.uk; Fax: 0044 121 414 4403*
[b] *School of Physics and Astronomy, University of Birmingham, Edgbaston, Birmingham, UK B15 2TT*
† The HTML version of this article has been enhanced with additional colour images.

electron from the neutral molecule, c-C_4F_8, to the cation. Fragmentation of c-$C_4F_8^+$ may then follow. Charge transfer can occur *via* two extreme mechanisms. We consider first long-range charge transfer. When an ion (A^+) and a neutral (BC) approach under the influence of their charge-induced dipole interaction, at some point on their approach the electron jump can occur. If this happens at a separation, *ca.* 5 Å, which is large compared to the size of such molecules, then the process is classed as long-range charge transfer. In this mechanism, BC acts as if isolated from A^+, and A^+ does not perturb the potential energy surface of BC. In essence, we are assuming that BC behaves as if it interacts with a photon, rather than a positively-charged particle. Previously, we have shown that the critical distance between A^+ and BC at which the jump occurs, R_c, depends on the difference between the recombination energy (RE) of A^+ and the ionisation energy (IE) of BC; the smaller this difference, the larger R_c becomes.[19] These facts suggest that, if long-range charge transfer occurs, then the product branching ratios from the ion-molecule and photoionisation reactions will be very similar. These two reactions can be summarised as follows:

$$A^+ + BC \rightarrow A + BC^{+\,(*)}; BC^{+\,(*)} \rightarrow \text{fragments}$$

$$h\nu + BC \rightarrow BC^{+\,(*)} + e^-; BC^{+\,(*)} \rightarrow \text{fragments}$$

If long-range charge exchange does not occur, then A^+ and BC move closer together. At a smaller separation, charge transfer may become favourable due to perturbation of the potential energy surface of BC by A^+, and BC can then be ionised. Under these circumstances, BC can no longer be assumed to be isolated, and it is therefore unlikely to fragment *via* the same pathways as those due to photoionisation. We call this process short-range charge transfer. We should note that these two mechanisms are extreme examples of charge transfer, but both can only occur when charge transfer is energetically favourable; that is, RE (A^+) must exceed IE (BC). A third possible mechanism for ion-molecule reactions is that a chemical reaction occurs. Here A^+ and BC form an intimate complex where bond making and breaking take place. Unlike either charge-transfer mechanism, there is no parent ion of BC formed as an intermediate which then fragments, and furthermore there is no necessity that RE (A^+) > IE (BC). Such chemical reactions can occur in competition with, or instead of, charge transfer.

2. Experimental

The apparatus used for the TPEPICO study has been described in detail previously.[20] The experiments were performed at the Daresbury SRS on station 3.2 using the 5 m McPherson monochromator, range *ca.* 10–25 eV at an optimum resolution of 0.025 nm.[21] With the grating used in these experiments, second-order radiation is insignificant for $h\nu$ > 13 eV, reaching a maximum of *ca.* 10% for lower photon energies. We see no evidence for second-order effects in this study. The synchrotron radiation is coupled into the reaction region *via* a capillary, and the flux is subsequently monitored by a photomultiplier tube through a sodium salicylate window. Threshold photoelectrons and fragment cations are extracted in opposite directions by an electric field of 20 V cm^{-1}. The electrons are detected in a threshold analyser with resolution *ca.* 10 meV, the ions in a linear time-of-flight (TOF) mass spectrometer with a resolution $m/\Delta m$ of *ca.* 200. The signals are detected by a channeltron and a pair of microchannel plates, respectively. The raw data pulses are discriminated and pass to a time-to-digital convertor. The electrons provide a start to the TOF detection window and the ions provide a stop, allowing signals from the same ionisation event to be detected in coincidence. Spectra are measured as a function of photon energy, where the data are recorded as 3-D maps of coincidence count *vs.* ion TOF *vs.* photon energy. These spectra can yield either the TOF mass spectrum at any photon energy or the yield of any fragment ion as a function of energy. Extraction of product branching ratios as a function of photon energy is facile, and in addition the threshold photoelectron spectrum is recorded as part of the coincidence experiment. It is also possible to record TOF spectra at higher resolution yielding kinetic energy releases, but these measurements were not made.

The SIFT technique has been reviewed in detail,[22,23] and full details of the current mode of operation of the Birmingham apparatus are given elsewhere.[24] Briefly, the apparatus consists of an ion source where neutral gases are ionised under high pressure by 70 eV electron ionisation. The required ion is selected using a quadrupole mass filter before being admitted into the flow tube, where it is carried along by a flow of high purity (99.997%) helium gas at a pressure of *ca.* 0.5 Torr. The neutral reagent is then injected downstream into the flow tube *via* one of two different inlets. Any resultant ionic products are detected by a quadrupole mass spectrometer. The amount of injected neutral is varied from zero to a value which depletes the reactant ion signal by *ca.* 90%. The loss of reagent ion and the increase in product ions are recorded as a function of neutral reagent concentration under pseudo-first order conditions. The error in the rate coefficient determined from the analysis is 20%,[22] and we are limited to measuring reactions with rate coefficients greater than *ca.* 10^{-13} cm^3 $molecule^{-1}$ s^{-1}. Branching ratios are derived from plots of ion signal *vs.* neutral concentration, and extrapolation to zero flow of the neutral molecule allows for the effects of secondary reactions. We quote an error of 15% in product branching ratios, this error increasing for values below 10%.

c-C_4F_8 was obtained from Fluorochem UK with a stated purity of 99%, and was used without further purification.

3. *Ab initio* molecular orbital calculations

To aid interpretation of results, we have calculated both the structure and molecular orbitals (MO) of c-C_4F_8 using Gaussian 03.[25] The structures were optimised from experimental, gas-phase electron diffraction data[11] at the MP2 level of theory using the 6-311-G+(d,p) basis set. Using this optimised structure, calculations of the ionisation energies were also performed using the outer-valence Green's Function (OVGF) method at the Hartree Fock level of theory. The geometry of the molecule is non-planar and puckered with D_{2d} symmetry, similar to that of the non-fluorinated cyclobutane molecule. In a previous study of ion and photon reactions with

CHF_3,[26] we were able to interpret results of some charge-transfer reactions by reference to the nature of the MOs of CHF_3 at energies corresponding to the RE of the cations. In all MOs it was possible to localise the electron density in specific regions/bond(s) of the molecule. In this study of *c*-C_4F_8, however, due to its greater size such simple interpretations have not been possible. The nature of the highest occupied MO of *c*-C_4F_8 at *ca.* 12 eV is easy to define, F 2pπ non-bonding with some C−C anti-bonding character. However, the complexity of MOs at higher energy in the range *ca.* 14–20 eV is much greater. It is almost impossible to define in a particular MO a localisation of electron density in one part of the molecule; if intramolecular energy redistribution is slow, such localisation can lead to a specific fragmentation route.[20,26] Whilst these calculations have therefore assisted in the assignment of the photoelectron spectrum of *c*-C_4F_8, they have not been able to assist in the interpretation of charge transfer reactions with cations of known RE.

4. Energetics

The energetics of the photodissociation channels of *c*-C_4F_8 are listed in Table 1. The appearance energies (AE_{298}) are measured from the first onset of signal above the background noise for each fragment. At the resolution and step size used in these experiments, this is equivalent to extrapolation of the linear portion of the ion yield to zero signal, and more sophisticated fitting procedures for the threshold region are not appropriate. The AE_{298} values can be converted into an upper limit for $\Delta_r H^0_{298}$, the enthalpy change for the corresponding unimolecular reaction, using the procedure of Traeger and McLoughlin,[27] a methodology discussed in detail elsewhere.[28] The upper limit arises due to the possible presence of an exit-channel barrier and/or a kinetic shift; if both are zero, the conversion is exact. This procedure does not apply to the parent ion, is only strictly applicable for fragmentations involving a single-bond cleavage, and was developed for interpretation of photoionisation yields rather than state-selected TPEPICO yields. Although the two fragment ions observed with greatest intensity, $C_3F_5^+$ and $C_2F_4^+$, involve multiple-bond cleavage, we have applied this correction factor to these two ions, noting that this is only as an approximation to aid in the interpretation of results. The enthalpies of formation at 298 K were taken from the standard sources,[29–31] apart from values for *c*-C_4F_8 (−1515 kJ mol^{-1}),[32] C_3F_5 (−729 kJ mol^{-1}) and $C_3F_5^+$ (+45 kJ mol^{-1}),[33] and CF_3 (−466 kJ mol^{-1}) and CF_3^+ (406 kJ mol^{-1}).[34] Any other values used to interpret results from the SIFT experiment, which are not given in these standard sources, are quoted in footnotes to Table 2. The recombination energies (RE) of the ions for the SIFT study, equivalent to the adiabatic ionisation energy of the corresponding neutral molecule, are given in column 1 of Table 2. These values also come from the standard sources,[29–31] except the values used for CF_3^+ (9.04 eV)[34] and SF_5^+ (9.78 eV).[35]

5. Calculation of reaction rate coefficients

We have performed calculations to determine the rate coefficients of all the ion-molecule reactions studied. These are shown in column 2 of Table 2. These collisional rate coefficients, shown in squared brackets, were calculated using modified averaged dipole orientation (MADO) theory,[36,37] which in the case of non-polar *c*-C_4F_8 reduces to the classic Langevin value.[38] Its value depends on the polarisability volume of the neutral, the charge on the ion and the reduced mass of the collision partners. The polarisability volume, α, for *c*-C_4F_8 was taken from a semi-empirical calculation, 1.25×10^{-29} m^3.[5] A second theoretical rate coefficient, shown in curved brackets, was calculated assuming that *c*-C_4F_8 has a quadrupole moment, Θ, using the parameterised collisional rate equation of Bhowmik and Su.[39] More details are given in section 6.2.1. For all reactions, the ions were assumed to be fully thermalised and in their ground vibrational and electronic states. The ratio of the experimental, k_{exp}, to the calculated, k_{calc}, rate coefficient defines the efficiency of the reaction. Since the Langevin model is classical and assumes that every collision between ion and neutral leads to reaction, k_{calc} is an upper limit to the rate coefficient of reaction, and the efficiency should not exceed unity.

6. Results and discussion

6.1 Results from the threshold photoelectron photoion coincidence study

6.1.1 Threshold photoelectron spectrum. The threshold photoelectron spectrum (TPES) of *c*-C_4F_8 was recorded from 11–25 eV with a resolution of 0.3 nm (Fig. 1). Although the resolution is not improved upon our earlier Daresbury study since the widths of the peaks are molecule-limited,[17] the

Table 1 Thermochemistry of the observed dissociative ionisation pathways of *c*-C_4F_8 at 298 K

	AE_{298}[a]/eV	$\Delta_r H^0_{298,exp}$[b]/eV	$\Delta_r H^0_{298,calc}$[c]/eV
Products of *c*-C_4F_8 (−1515)[d]			
c-$C_4F_8^+$ (−396)[e] + e^-	11.60		
$C_3F_5^+$ (45) + CF_3 (−466) + e^-	11.68	11.95[f]	11.33
$C_2F_4^+$ (316) + C_2F_4 (−659) + e^-	11.86	12.13[f]	12.15
CF^+ (1134) + C_3F_7 (−1335) + e^-	14.7		13.62
CF_2^+ (922) + C_3F_6 (−1125) + e^-	15.0		13.60
CF_3^+ (406) + C_3F_5 (−729) + e^-	15.4		12.36

[a] Experimentally derived appearance energies, measured from onset of signal above noise. [b] Experimentally measured upper limit for enthalpy of unimolecular reaction, derived using the method of Traeger and McLoughlin.[27] [c] Calculated value for enthalpy of reaction given by literature values of enthalpy of formation of products minus that of reactants. [d] Literature values for $\Delta_f H^0_{298}$ are given in kJ mol^{-1} in brackets in column 1. [e] Value calculated from our experimental value for AE_{298}. [f] Approximate value as more than one bond is broken in dissociation (see section 4).

Table 2 Rate coefficients at 298 K, product cations and branching ratios, and suggested neutral products[a] for reactions of gas-phase cations with *c*-C_4F_8. The calculated enthalpy of reaction at 298 K is shown in the fifth column. The dotted line shows the position of the onset of ionisation of *c*-C_4F_8, 11.60 eV

Reagent ion (RE[b]/eV	Rate coefficient[c]/10^{-9} cm^3 molecule^{-1} s^{-1}	Product ions (%)	Proposed neutral products	$\Delta_r H^0_{298}$/kJ mol^{-1}
H_3O^+	—	No reaction[d]	—	—
(6.27)	[2.0]/(2.5)			
SF_3^+	—	No reaction	—	—
(8.32)	[1.1]/(1.3)			
CF_3^+	—	No reaction	—	—
(9.04)	[1.2]/(1.5)			
CF^+	—	No reaction	—	—
(9.11)	[1.6]/(2.0)			
NO^+	—	No reaction	—	—
(9.26)	[1.6]/(2.1)			
SF_5^+	—	No reaction	—	—
(9.78)	[0.9]/(1.2)			
SF_2^+	—	No reaction	—	—
(10.24)	[1.1]/(1.5)			
SF^+	—	No reaction	—	—
(10.31)	[1.3]/(1.7)			
CF_2^+	1.3	$C_4F_7^+$ (60)	CF_3	−39[e]
(11.44)	[1.3]/(1.7)	$C_4F_6^+$ (15)	CF_4	−361
		CF_3^+ (25)	*c*-C_4F_7	−167
			$C_3F_3 + CF_4$	−68
			$C_3F_4 + CF_3$	−61
SF_4^+	—	No reaction	—	—
(11.99)	[1.0]/(1.3)			
O_2^+	1.9	*c*-$C_4F_8^+$ (1)	O_2	−46
(12.07)	[1.6]/(2.0)	$C_3F_5^+$ (51)	$O_2 + CF_3$	−844
			$COF_2 + OF$	−908
		$C_2F_4^+$ (48)	$O_2 + C_2F_4$	8
			$COF_2 + COF_2$	−611
Xe^+	1.3	*c*-$C_4F_8^+$ (2)	Xe	−51
(12.13/13.44)	[0.9]/(1.2)	$C_3F_5^+$ (41)	$Xe + CF_3$	−77
		$C_2F_4^+$ (57)	$Xe + C_2F_4$	2
H_2O^+	2.4	$C_3F_5^+$ (51)	$COF + 2HF$	−136
(12.62)	[2.0]/(2.6)		$CF_3 + H_2O$	−123
			$COF_2 + HF + H$	−109
			$CHF_3 + OH$	−74
		$C_2F_4^+$ (49)	$CH_2F_2 + COF_2$	−234
			$O(CHF_2)_2$	−228
			$CHF_3 + HF + CO$	−224
			$CHF_3 + HFCO$	−218
			$CF_4 + H_2CO$	−193
N_2O^+	2.2	$C_3F_5^+$ (30)	$COF_3 + N_2$	−397
(12.89)	[1.4]/(1.7)		$COF_2 + F + N_2$	−326
			$CF_3 + N_2O$	−150
		$C_2F_4^+$ (70)	$CF_4 + CO + N_2$	−539
			$C_2F_4O + N_2$	−499
O^+	2.3	$C_3F_5^+$ (25)	CF_3O	−634
(13.62)	[2.1]/(2.7)		$CF_2O + F$	−563
			$CF_3 + O$	−220
		$C_2F_4^+$ (75)	C_2F_4O	−736
			$CF_2O + CF_2$	−553
CO_2^+	1.7	$C_3F_5^+$ (22)	$CF_3 + CO_2$	−235
(13.76)	[1.4]/(1.8)		$COF_2 + COF$	−190
			$COF_3 + CO$	−117
		$C_2F_4^+$ (78)	$CF_4 + 2CO$	−258
			$C_2F_4O + CO$	−218
Kr^+	1.3	$C_3F_5^+$ (14)	$CF_3 + Kr$	−257
(14.00)	[1.1]/(1.4)	$C_2F_4^+$ (86)	$C_2F_4 + Kr$	−178
CO^+	2.0	$C_3F_5^+$ (20)	CF_3CO	−290
(14.01)	[1.7]/(2.1)		$CF_3 + CO$	−258
		$C_2F_4^+$ (80)	$C_2F_4 + CO$	−179
N^+	2.8	$C_4F_8^+$ (1)[f]	N	−427
(14.53)	[2.3]/(2.9)	$C_3F_5^+$ (41)	$CF_3 + N$	−309
			$FCN + F_2$	−280
			$CF_2 + NF$	−249
		$C_2F_4^+$ (58)	$CF_4 + CN$	−542
			$CF_3 + FCN$	−474
			$CF_3CN + F$	−460
			$C_2F_4 + N$	−230

Table 2 (*continued*)

Reagent ion (RE[b]/eV	Rate coefficient[c]/10^{-9} cm^3 molecule^{-1} s^{-1}	Product ions (%)	Proposed neutral products	$\Delta_f H^0_{298}$/kJ mol^{-1}
N_2^+	2.2	$C_4F_7^+$ (9)	F + N_2	−74[e]
(15.58)	[1.7]/(2.1)	$C_3F_6^+$ (1)	CF_2 + N_2	−272
		$C_3F_5^+$ (16)	CF_3 + N_2	−410
		$C_2F_4^+$ (74)	C_2F_4 + N_2	−331
Ar^+	1.8	$C_4F_7^+$ (22)	F + Ar	−92[e]
(15.76)	[1.4]/(1.8)	$C_3F_6^+$ (1)	CF_2 + Ar	−290
		$C_3F_5^+$ (20)	CF_3 + Ar	−428
		$C_2F_4^+$ (57)	C_2F_4 + Ar	−349
F^+	2.3	$C_4F_7^+$ (3)	F_2	−410[e]
(17.42)	[2.0]/(2.5)	$C_3F_5^+$ (38)	CF_4	−1133
		$C_2F_4^+$ (49)	C_2F_5	−822
			CF_4 + CF	−607
			CF_3 + CF_2	−577
			C_2F_4 + F	−508
		CF_3^+ (10)	C_3F_6	−964
			C_2F_4 + CF_4	−751
Ne^+	2.5	$C_4F_7^+$ (1)	F + Ne	−651[e]
(21.56)	[1.9]/(2.5)	$C_4F_6^+$ (1)	F_2 + Ne	−586
		$C_3F_5^+$ (31)	CF_3 + Ne	−987
		$C_3F_4^+$ (1)	CF_4 + Ne	−1042
		$C_2F_4^+$ (25)	C_2F_4 + Ne	−908
		$C_2F_3^+$ (1)	C_2F_5 + Ne	−667
		CF_3^+ (31)	C_3F_5 + Ne	−888
		CF_2^+ (6)	C_3F_6 + Ne	−768
		CF^+ (3)	C_3F_7 + Ne	−766

[a] The majority of the enthalpies of formation at 298 K for ion and neutral species are taken from standard sources.[29–31] Exceptions are more recent experimental values for CF_3 (−466 kJ mol^{-1}) and CF_3^+ (406 kJ mol^{-1}),[34] *c*-C_4F_7 (−1166 kJ mol^{-1}) and *c*-$C_4F_7^+$ (−166 kJ mol^{-1}),[40] C_3F_3 (−134 kJ mol^{-1}),[33] $O(CHF_2)_2$ (−858 kJ mol^{-1}),[46] CF_3O (−631 kJ mol^{-1}) and CF_3CO (−609 kJ mol^{-1}),[47] and C_2F_4O (−1004 kJ mol^{-1}).[48] [b] Recombination energy (RE) of reactant ion. For molecular ions, the RE is given for $v^+ = 0$. Data taken from standard sources,[29–31] except values used for CF_3^+ (9.04 eV)[34] and SF_5^+ (9.78 eV).[35] [c] The values in square brackets are calculated by the Modified Average Dipole Orientation model,[36,37] using literature values for the polarisability of *c*-C_4F_8.[5] The values in curved brackets are the rate coefficients calculated using the quadrupole method of Bhowmik and Su for a value of $\Theta = 7.0 \times 10^{-39}$ C m^2.[39] [d] No reaction means the rate coefficient is less than *ca.* 10^{-13} cm^3 molecule^{-1} s^{-1}. [e] Assuming ion is cyclic-$C_4F_7^+$. [f] Due to the higher RE of N^+ we assume that $C_4F_8^+$ is formed here in the linear isomeric form.

signal-to-noise ratio is superior, reflecting the enhanced performance of the 5 m McPherson over the 1 m Seya monochromator. The onset of ionisation was determined to be 11.60 ± 0.05 eV, in excellent agreement with our previous study[17] but significantly lower than the value of 12.25 eV from an early electron ionisation study.[7] This discrepancy is probably due to the inherent inferior resolution of electron ionisation, and the method used to determine appearance energies by extrapolation with reference to the onset of ionisation for argon.[7] As described in section 3, we have calculated the valence MOs of *c*-C_4F_8 at the MP2 level. In D_{2d} symmetry they are labelled ... $(9a_1)^2$ $(9e)^4$ $(1a_2)^2$ $(8b_2)^2$ $(10e)^4$ $(10a_1)^2$ $(9b_2)^2$ $(2b_1)^2$ $(11e)^4$ $(11a_1)^2$ $(12e)^4$ $(3b_1)^2$, where the numbering includes all atomic orbitals. The ionisation energies have then been calculated by the OVGF method. There are more molecular orbitals than resolved peaks in the TPES of Fig. 1; this is obviously due to the resolution not being sufficient to resolve the separate states. In Fig. 1 the state labelled $\tilde{X}$ refers to ionisation from the HOMO of symmetry B_1. The vertical ionisation energy of this peak, 12.4 eV, is in good agreement with the OVGF calculation of 12.1 eV, and the HOMO is mainly F 2pπ non-bonding with some C–C anti-bonding character. The peak at 14.0 eV, corresponding to ionisation to the $\tilde{A}$ ^2E state of *c*-$C_4F_8^+$, is in excellent agreement with the OVGF calculation. At higher energies, the peaks are unresolved combinations of various molecular orbitals. In particular, the next ten orbitals in *c*-C_4F_8 are calculated to have energies in the range 16.4–18.3 eV, incorporating the three resolved peaks at 16.2, 17.0 and 17.8 eV labelled $\tilde{B}$, $\tilde{C}$, $\tilde{D}$ in Fig. 1. Since the OVGF energies are calculated only at the Hartree Fock level, there are small changes in ordering of these ten orbitals compared to the ordering at the MP2 level. The peaks between 19 and 21 eV are

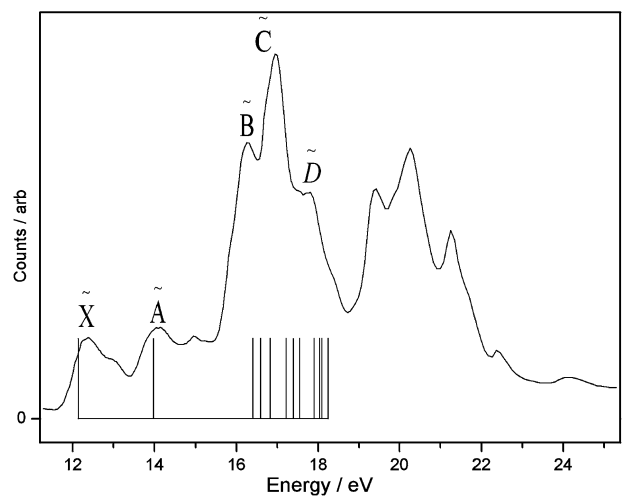

Fig. 1 Threshold photoelectron spectrum for *c*-C_4F_8 in the energy range 11–25 eV at a resolution of 0.3 nm. The stick spectrum represents the ionisation energies of the twelve highest orbitals calculated by the outer valence green function method.

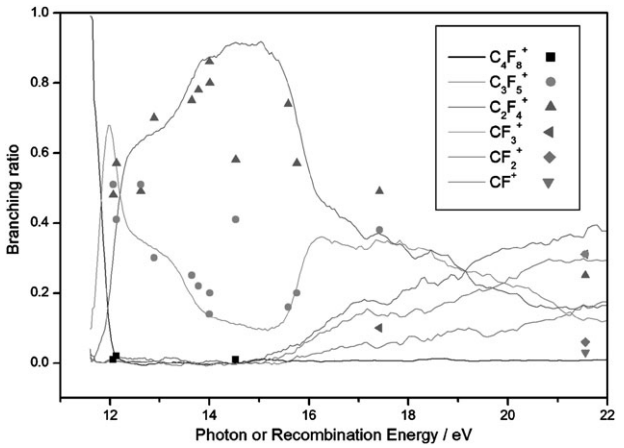

Fig. 2 Comparison of product ion branching ratios from photon-induced TPEPICO spectroscopy with those from ion-molecule studies of *c*-C_4F_8 over the energy range 11.6–22.0 eV. The former data appear as continuous lines, the latter data as individual points at the recombination energy of the ion. For clarity, product ions whose yield is zero from the ion-molecule study are not shown. (The HTML version of this figure has been enhanced with colour.)

not assigned since the OVGF method does not allow for the calculation of ionisation energies above 20 eV. Weak peaks at 12.8 and 14.8 eV may be due to autoionisation of Rydberg states of *c*-C_4F_8. Such peaks would be absent in a direct-ionisation He I photoelectron spectrum, but such a spectrum is not available for comparison.

6.1.2 Scanning threshold photoelectron photoion coincidence spectra. The scanning-energy TPEPICO spectrum was also recorded for *c*-C_4F_8 from 11–25 eV with an optical resolution of 0.3 nm and a TOF resolution of 64 ns. This TOF resolution is inferior to the optimum resolution of the time-to-digital converter, but all product ions could then be seen on one 3-D coincidence scan while still obtaining unambiguous identification of the products. Six ions were observed, $C_4F_8^+$, $C_3F_5^+$, $C_2F_4^+$, CF^+, CF_2^+ and CF_3^+, and Table 1. Column 2 lists their appearance energies. The breakdown diagram over this energy range is shown as continuous solid lines in Fig. 2. Whilst there are no major differences from that reported in our earlier study,[17] the improved statistics of the present coincidence map mean that this diagram is more accurate. The signal from $C_4F_8^+$ is very weak above its threshold energy for production. As its intensity reduces, $C_3F_5^+$ and $C_2F_4^+$ are the two main fragment ions observed. The smaller three cations turn on at higher energy and are much weaker. The onset of ionisation is determined to be 11.60 eV ± 0.05. For dissociation of the parent ion into $C_3F_5^+$ and $C_2F_4^+$, the appearance energies of 11.68 ± 0.05 and 11.86 ± 0.05 eV have been converted into $\Delta_r H^0_{298}$ values of the corresponding unimolecular reactions; it is assumed that the neutral products are CF_3 and C_2F_4, respectively. The onsets for production of CF^+, CF_2^+ and CF_3^+ are less well defined, and their onsets are quoted with an error in each value of ±0.2 eV.

Although the parent ion has been observed with 0.1% relative abundance in a 70 eV electron ionisation mass spectrum,[30] this is the first time that the parent ion has been detected by photoionisation, and $C_4F_8^+$ is only observed over a very narrow energy range, *ca.* 11.6−12.2 eV. This suggests that the experiment is only sampling a small bound region of the $\tilde{X}$ state of $C_4F_8^+$ in an otherwise unbound potential energy surface. We note that the *ab initio* calculations predict a singly-degenerate state of $^2B_1$ symmetry for the ground state of $C_4F_8^+$. Whilst higher-lying electronic states of $C_4F_8^+$ will have orbital degeneracy, and hence are susceptible to Jahn–Teller distortion and possible fragmentation, this argument is not valid for the ground state. In an *ab initio* study of the energetics and decomposition pathways of *c*-$C_4F_8^+$,[40] Bauschlicher and Ricca calculated an adiabatic (vertical) ionisation energy for *c*-C_4F_8 of 10.76 (11.24) eV, respectively. These values are significantly lower than previous experimental values[7,17] and this study. They also showed that the open chain, linear isomer of $C_4F_8^+$ lies *ca.* 7 kJ mol^{-1} below the initially-formed cyclic form, with a barrier, B1, linking its two isomers (Fig. 3). Furthermore, vertical excitation from the ground state of *c*-C_4F_8 will form the ion above this barrier, and several possible fragmentation pathways are then available. Our result, that $C_3F_5^+$ and $C_2F_4^+$ are observed as the lowest-energy fragment ions, agrees with their calculations. Although the calculated ionisation energies of Bauschlicher and Ricca disagree with experimental data, the *relative* energies of the fragmentation pathways of *c*-$C_4F_8^+$ are more likely to be valid. With our experimental data as an absolute energy scale, we will therefore use these calculations to aid interpretation of our results.

We assume that $C_4F_8^+$ observed over the photon range *ca.* 11.6–12.2 eV is cyclic, and not linear. From the theoretical study,[40] the barrier B1 must be surmounted for cyclic-$C_4F_8^+$ to isomerise to the linear form. B1 is calculated to lie less than 10 kJ mol^{-1} below the barrier, B2, that leads to fragmentation to $C_3F_5^+ + CF_3$ following a 1,3 fluorine-atom migration. So, if the photoionisation energy is sufficient to overcome B1, it is probably sufficient also to overcome B2 and fragment the parent ion. There is a small range of energies, 11.60–11.68 eV, where parent ions but not $C_3F_5^+$ are observed. We believe this is strong evidence that the parent ion in this range can only exist in the cyclic form.

The main fragments formed between 11.6 and 16.0 eV are $C_3F_5^+$ and $C_2F_4^+$. Following the decrease in the parent ion signal above threshold, $C_3F_5^+$ is the first fragment ion to be observed, onset 11.68 eV. The threshold for $C_2F_4^+$ production is slightly higher, 11.86 eV, and this ion is dominant in the energy range 12.5–17.5 eV. Between 14 and 16 eV, the yield of $C_3F_5^+$ falls, before increasing again as the Franck–Condon envelope of the $\tilde{B}$-state peak at 16.2 eV is attained (Fig. 1). Above 14.5 eV, the small CF_x^+ (x = 1, 2 and 3) series of ions form, and by *ca.* 20 eV they are the dominant fragment ions. Formally, as described earlier, the method of Traeger and McLoughlin[27] cannot be applied to any of the fragmentation pathways we detect. However, we have applied this procedure to pathways which form both $C_3F_5^+$ and $C_2F_4^+$; it is assumed that the neutral partners are CF_3 and C_2F_4, respectively. The corrections to the AE_{298} values were estimated from well-known vibrational frequencies for CF_3 and C_2F_4,[29,41] with Gaussian 03 calculations at the B3LYP 6-311-G+(d,p) level providing values for $C_3F_5^+$ and $C_2F_4^+$. These approximate

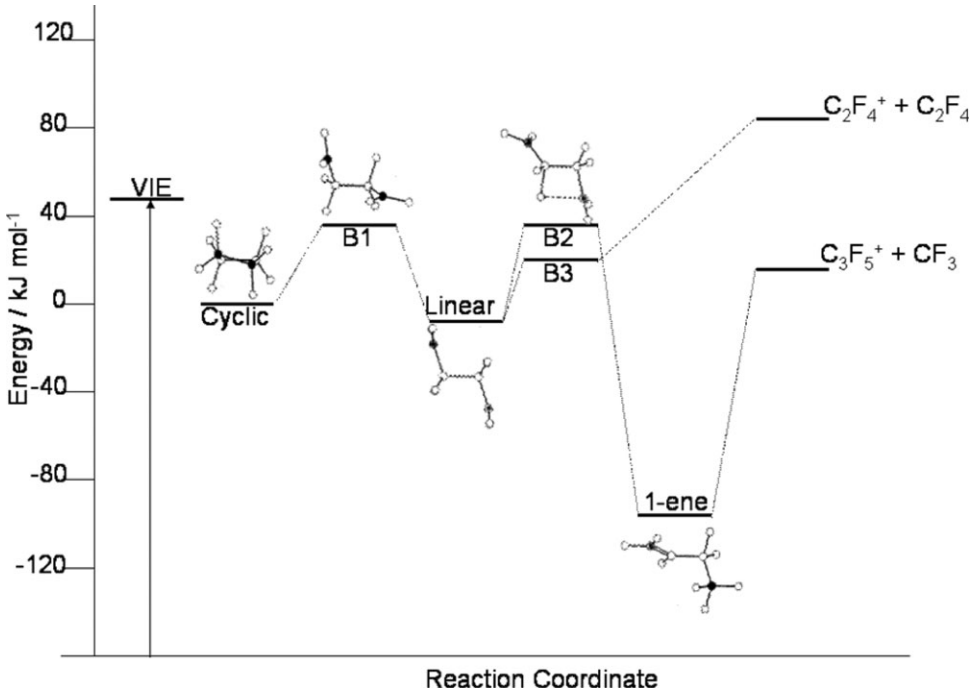

Fig. 3 Pathways for fragmentation of c-$C_4F_8^+$, adapted with permission from ref. 40. The units of energy on the y-axis are kJ mol^{-1}, all referenced to a zero level corresponding to the lowest vibrational level of c-$C_4F_8^+$. VIE refers to the vertical ionisation energy from the ground state of neutral c-C_4F_8.

values for $\Delta_r H^0_{298}$ of the unimolecular reactions allow us to make some statements about the fragmentation dynamics.

We consider first c-$C_4F_8 \rightarrow C_3F_5^+ + CF_3 + e^-$. The calculated and experimental $\Delta_r H^0_{298}$ values (Table 1) show that the threshold for this channel occurs *ca.* 0.6 eV above the thermochemical threshold, suggesting the presence of a barrier in the exit channel. This is to be expected as the fragmentation mechanism must involve an intramolecular 1,3 F-atom transfer. This requires alignment of the fluorine atom with an orbital on the accepting carbon atom before transfer can take place, which is unlikely to be a barrier-free process. For the fragmentation c-$C_4F_8 \rightarrow C_2F_4^+ + C_2F_4 + e^-$, two mechanisms are possible; a concerted process, effectively an inverse cycloaddition, or a sequential scissoring of the two C−C bonds. On the basis of frontier molecular orbitals,[42] the concerted mechanism is forbidden. This means that only the second mechanism is valid, and fragmentation must go through a radical intermediate. Our results show that the reaction occurs at the thermochemical threshold (Table 1), so there can be no barrier in this exit channel. These interpretations are in agreement with the study of Bauschlicher and Ricca.[40] In their calculations $C_3F_5^+$ is only formed after barrier B2 (Fig. 3), which is the transition state where the fluorine and carbon atoms align themselves for the 1,3 F-atom migration, is surmounted. $C_3F_5^+$ therefore forms above its thermochemical threshold; using Gaussian 98 at the G3MP2 level of theory, this difference is calculated to be 0.31 eV.[40] This study also calculated a transition state in the pathway to formation of $C_2F_4^+$, B3 (Fig. 3). However, since this transition state lies below the thermochemical threshold, $C_2F_4^+$ is indeed observed to have an appearance energy at its thermochemical threshold.

The first appearance of $C_3F_5^+$ at an energy significantly higher than its thermochemical threshold can be regarded as a manifestation of non-statistical behaviour, in which dissociation occurs only along specific potential energy pathways.[20] The further rise in the $C_3F_5^+$ signal at *ca.* 15.5 eV (Fig. 2) corresponds to the rise in the threshold electron signal of the $\tilde{B}$ state of c-$C_4F_8^+$, suggesting that this state also fragments non-statistically. Noting that the appearance energies of CF_x^+ are all significantly greater than the lowest thermochemical threshold (Table 1), the simultaneous rise in the yields of these ions at this energy also suggests that they result from state-selected fragmentation of the $\tilde{B}$ state of c-$C_4F_8^+$. We have no evidence whether CF_x^+ forms sequentially from secondary fragmentation of $C_3F_5^+$ or directly. The theoretical study[40] suggests that CF_3^+ does form directly from $C_4F_8^+$ *via* B2, although the authors do not rule out a competing secondary process.

6.2 Results from the selected ion flow tube study

6.2.1 Rate coefficients. A major discrepancy is observed between the experimental rate coefficients and those calculated using MADO theory; the experimental rates are larger than the predicted collisional rates, to an extent that is greater than the experimental error. We assume that the values for k_{exp} are correct because there is excellent agreement of our data with that of an earlier SIFT study by Morris *et al.*[16] who state that their values for k_{exp} occur at the collisional rate. Since no details are given of how their calculations are performed, we assume that there is an error in our simple calculations. In our study, the value used for the polarisability volume of c-C_4F_8 is the largest of several values which are available in the

literature.[5] Although this gives better agreement with experiment than lower values of α, k_{calc} is still significantly smaller than k_{exp} for all reactions. One reason for this discrepancy may be that c-C_4F_8 has another ion-neutral interaction which has not been taken into account. Any additional attractive interaction would lead to an increase in the intermolecular potential and hence in the rate of collisions. It cannot be an ion–dipole interaction as c-C_4F_8 is a highly symmetrical molecule with no permanent dipole moment. However, a significant quadrupole moment of c-C_4F_8 would increase the rate of reaction. Rate coefficients have therefore been recalculated using the parameterized formula of Bhowmik and Su,[39] where one additional parameter to the original Langevin theory is the quadrupole moment of the neutral molecule. Since no value for Θ of c-C_4F_8 exists in the literature, we have used a value of $7.0 \pm 0.7 \times 10^{-39}$ C m^2. This empirical value and associated error gives values for the rate coefficients of a large number of the ion reactions studied which agree with the experimental values within error. The mean value for Θ, 7.0×10^{-39} C m^2, was determined by the fact that it gives a value for k_{calc} of $Ne^+ + c$-C_4F_8 which is in exact agreement with the experimental rate coefficient; it is assumed that Ne^+ reacts at the collisional, *i.e.* capture rate. A calculation of Θ at the MP2 level of theory gives a similar value, 7.3×10^{-39} C m^2. However, it has been suggested that these values are too high,[43] based on a comparison to the quadrupole moment of C_6F_6 in the gas phase, 2.8×10^{-39} C m^2,[44] which should have a larger quadrupole moment than c-C_4F_8. Nevertheless, the value we use allows us to make qualitative comparisons and statements on the efficiency of the reactions and compare the different results.

Using our value for Θ, with two exceptions all reactions proceed at the collisional rate. The two exceptions are CF_2^+ and N_2O^+. CF_2^+ reacts with an efficiency of only 75%. Since the RE (CF_2^+) is less than the IE (c-C_4F_8), this reaction can only proceed *via* an intimate chemical pathway, and steric effects may play a role. We note that this is the only ion with RE below IE (c-C_4F_8) where reaction is observed. N_2O^+ has an experimental rate coefficient 30% higher than the calculated value incorporating an ion–quadrupole interaction. This is outside experimental error, and we can offer no explanation for this large value.

6.2.2 Branching ratios. Table 2 displays the experimental and calculated rate coefficients (column 2) and the ionic products and their branching ratios from the SIFT study (column 3). Proposed neutral products (column 4) and the corresponding enthalpies of reaction (column 5) are also shown. The proposed pathways are those which are both chemically feasible and have the most negative values for $\Delta_r H^0_{298}$. In cases where there are several feasible pathways, we only present an indicative selection.

CF_2^+ is the only ion with RE < IE (c-C_4F_8) which reacts. Three ionic products, $C_4F_7^+$ (60%), $C_4F_6^+$ (15%) and CF_3^+ (25%) are observed, and there are exothermic channels for their production which involve the loss of one or more fluorine atoms from c-C_4F_8. We should note that CF^+ is also present in the flow tube, almost certainly produced by collision-induced dissociation of CF_2^+, but since this ion does not react with c-C_4F_8 its presence at the detection quadrupole mass spectrometer as a background signal poses no problem. Jiao *et al.*[15] have also studied the reaction of CF_2^+ with c-C_4F_8 in an ion cyclotron resonance Fourier transform mass spectrometer (ICR-FTMS). For their study $C_3F_5^+$ is the major product, 53%, with $C_4F_7^+$, $C_4F_6^+$, $C_2F_4^+$ and CF_3^+ as minor products. Whilst exothermic channels involving $C_3F_5^+$ do exist, this product ion is absent as a product in the SIFT experiment. An explanation can be provided by the different conditions between the SIFT and ICR experiments. Translational energies are thermalised in SIFT studies, whereas in an ICR there is more uncertainty in the kinetic energy of the ions. This has led to differences in both measured ion branching ratios and reaction rate coefficients in other studies.[45]

For ions with RE values above 11.60 eV, the onset of ionisation of c-C_4F_8, the mechanism of long-range charge transfer becomes energetically open. All bar SF_4^+ (RE = 11.92 eV) react with efficiency close to 100%. Exothermic pathways are available for the reaction of $SF_4^+ + c$-C_4F_8, and we can only assume that the reaction cross-section at this energy close to threshold is very small. For the remaining ions, a range of ionic products are observed. For ions with RE values up to *ca.* 15 eV, the major products are $C_3F_5^+$ and $C_2F_4^+$, and in addition the parent ion is observed weakly for reactions of O_2^+, Xe^+ and N^+. For ions with RE values above 15 eV, a larger range of fragment ions is observed ($C_4F_7^+$, $C_4F_6^+$, $C_3F_6^+$, $C_3F_4^+$ $C_2F_3^+$, CF_3^+, CF_2^+ and CF^+), the $C_3F_5^+$ and $C_2F_4^+$ branching ratios decrease, and the parent ion is not observed. The structure of the parent ion cannot be determined. As described in section 6.1.2, we assume that it takes the cyclic form for reactions of Xe^+ and O_2^+, but possibly it has the linear structure for the reaction with N^+ since the RE of this ion, 14.53 eV, lies above the barrier to isomerisation (Fig. 3).

The results of Smith and Kevan for reactions of c-C_4F_8 with noble gas cations agree broadly with our data.[14] However, in this study the ions have a much higher average kinetic energy of *ca.* 50 eV, which may explain why they observe greater fragmentation in their product ions. Jiao *et al.*[15] performed electron ionisation of c-C_4F_8 in an ICR-FTMS, isolated the products, and reacted them with the parent neutral, measuring rate coefficients and product branching ratios. Only two fluorocarbon fragments formed by electron ionisation, CF_2^+ and $C_2F_3^+$, reacted with c-C_4F_8. The results of the CF_2^+ reaction were discussed above, and we did not study the $C_2F_3^+$ reaction in the SIFT. Jiao *et al.* also studied the reactions of c-C_4F_8 with Xe^+, Kr^+ and Ar^+. The results for Kr^+ and Xe^+ are in good agreement with our data, but agreement is poor for Ar^+. Morris *et al.*[16] used a SIFT to study reactions of c-C_4F_8 with cations and anions of atmospheric importance. As stated earlier, our rate coefficients agree excellently but, whereas the O^+ product branching ratios are in reasonable agreement, those for O_2^+ are poor; they reported $C_3F_5^+$ and $C_2F_4^+$ in the ratio 72 : 28% and observe no parent ion, whereas our study observes this ratio as 51 : 48% with the additional presence of a weak parent ion signal, 1%. We comment that thermalisation of excited vibrational levels of O_2^+ does not always occur in a SIFT,[22] so several $O_2^+(v)$ levels may be contributing to the reaction with c-C_4F_8. This phenomenon can manifest as curvature in the pseudo-first-order rate

plot of ln(ion signal) *vs.* neutral concentration.[22] In our study, we observed no such curvature. However, we cannot rule out different amounts of $O_2^+(v)$ vibrational excitation in the two studies as contributing to the different product ion branching ratios.

7. Comparison of branching ratios from the TPEPICO and SIFT experiments

Fig. 2 shows the branching ratios from the TPEPICO and SIFT studies as a function of energy. The former appear as continuous graphs, whereas the latter appear as data points at defined RE values of the ion. We only include the fragment ions from the SIFT study which are observed in the TPEPICO experiments. As described in the Introduction, a comparison of the branching ratios may indicate the mechanism of the cation reactions, in particular whether a long-range charge transfer mechanism is operating. For ions with RE values in the range 11.6 to 12.6 eV (O_2^+, Xe^+ and H_2O^+), the agreement between the $C_3F_5^+$ and $C_2F_4^+$ branching ratios is poor, and exceeds the 15% error we define as evidence for long-range charge transfer.[26] Over this range, however, the TPEPICO branching ratios are changing very rapidly with photon energy, so this is a particularly severe test of agreement between the two sets of data. 12.6 eV corresponds to the high-energy end of the Franck–Condon region of the $\tilde{X}$ state of *c*-$C_4F_8^+$. The poor agreement between these datasets over this energy range may suggest that the orbitals involved in the ionisation process are shielded from the approaching ion, making long-range charge transfer an unfavourable process.[19,24,26] For ions with RE values in the range 12.9–15.8 eV, with the exception of N^+ (RE = 14.53 eV) the branching ratios into $C_3F_5^+$ and $C_2F_4^+$ agree well between the two experiments. We conclude that the reactions of N_2O^+, O^+, CO_2^+, Kr^+, CO^+, N_2^+ and Ar^+ all probably proceed by long-range charge transfer. The reactions of N^+ are often anomalous in our SIFT apparatus,[24,26] with branching ratios of fragment ions significantly different in the TPEPICO and SIFT studies. Since it is difficult to assign the MOs of *c*-C_4F_8 over this energy range to localisation of electron density in one part of the molecule, the *ab initio* calculations (section 3) have not been able to assist in the interpretation of why charge transfer reactions with cations in this range of RE values appear to take place at long range. For the two ions with RE greater than 16 eV, F^+ at 17.42 and Ne^+ at 21.56 eV, the agreement of the two datasets is poor again. For F^+, the difference in branching ratios could possibly be explained by the low signal of ion which can be formed in the high-pressure SIFT source, resulting in difficulties to obtain reliable branching ratios. For Ne^+, many more fragments are observed in the ion-molecule reaction than with photoionisation at 21.56 eV, so Ne^+ cannot react *via* a long-range mechanism. Since this inert rare gas ion cannot undergo chemical reactions, Ne^+ can only react by a short-range dissociative charge transfer mechanism (section 1).

8. Conclusions

The threshold photoelectron and threshold photoelectron photoion coincidence spectra of *c*-C_4F_8 in the range 11–25 eV have been recorded. The parent ion has been observed very weakly at threshold, 11.60 ± 0.05 eV, and it is most likely to have cyclic geometry. Ion yield curves and branching ratios have been determined above the ionisation threshold of *c*-C_4F_8 for the five fragments produced; $C_3F_5^+$, $C_2F_4^+$, CF^+, CF_2^+ and CF_3^+. The first ion formed is $C_3F_5^+$, at slightly higher energy $C_2F_4^+$, then successively CF^+, CF_2^+ and CF_3^+ are formed. The dominant ions are $C_3F_5^+$ and $C_2F_4^+$. It is assumed that the accompanying neutral fragments are CF_3 and C_2F_4, respectively. In agreement with calculations of Bauschlicher and Ricca,[40] we predict that there is a barrier in the exit channel for formation of $C_3F_5^+$, whilst there is no barrier for production of $C_2F_4^+$.

The branching ratios and rate coefficients have been measured in a selected ion flow tube at 298 K for the bimolecular reactions of *c*-C_4F_8 with H_3O^+, CF_x^+ (x = 1–3), SF_x^+ (x = 1–5), NO^+, O_2^+, Xe^+, H_2O^+, N_2O^+, O^+, CO_2^+, Kr^+, CO^+, N^+, N_2^+, Ar^+, F^+ and Ne^+. Below the energy where charge transfer becomes energetically allowed, *ca.* 11.6 eV, only one of the nine ions, CF_2^+, reacts. Above this energy, all but one of the fourteen remaining ions reacts. It has been difficult to comment on the reaction efficiency (k_{exp}/k_{calc}) due to k_{exp} values which are consistently greater than the collisional values calculated from modified average dipole orientation theory. The inclusion of an additional ion–quadrupole interaction with a sensible choice of quadrupole moment for *c*-C_4F_8 has allowed better agreement to be achieved. With the exception of N^+, a comparison of the fragment ion branching ratios from the TPEPICO and SIFT data suggest that long-range charge transfer is the dominant mechanism for reactions of ions with recombination energy between 12.9 and 15.8 eV. For all other ions, either short-range charge transfer and/or a chemical reaction occurs.

Acknowledgements

We thank EPSRC for grants GR/S21557 and GR/M42974 and the help of the staff of the Daresbury Laboratory, especially Dr Andrew Malins. We acknowledge Matthew Simpson for help with establishing the thermochemistry of the ion-molecule reactions. We are particularly grateful to Professor Charles Bauschlicher for permission to show a modified version of his calculated dissociation pathways of *c*-$C_4F_8^+$,[40] and we thank Professor Geoff Ritchie for discussions on quadrupole moments. MAP and SA thank the EPSRC Doctoral Training Account and the University of Birmingham, respectively, for studentships.

References

1 Y. Gotoh and T. Kure, *Jpn. J. Appl. Phys.*, 1995, **34**, 2132.
2 H. Kazumi and K. Tago, *Jpn. J. Appl. Phys.*, 1995, **34**, 2125.
3 K. Kubota, H. Matsumoto, H. Shindo, S. Shingubara and Y. Horiike, *Jpn. J. Appl. Phys.*, 1995, **34**, 2119.
4 C. A. Mayhew, A. D. J. Critchley, D. C. Howse, V. A. Mikhailov and M. A. Parkes, *Eur. Phys. J. D*, 2005, **35**, 307.
5 L. G. Christophorou and J. K. Olthoff, *Fundamental Electron Interactions with Plasma Processing Gases*, Kluwer Academic/Plenum Publishers, New York, 2004.
6 I. Sauers, L. G. Christophorou and J. G. Carter, *J. Chem. Phys.*, 1979, **71**, 3016.

7 M. M. Bibby and G. Carter, *Trans. Faraday Soc*., 1963, **59**, 2455.
8 A. Yokoyama, K. Yokoyama and G. Fujisawa, *Chem. Phys. Lett*., 1995, **237**, 106.
9 J. M. Simmie, W. J. Quiring and E. Tschuikow-Roux, *J. Phys. Chem*., 1969, **75**, 3830.
10 J. N. Butler, *J. Am. Chem. Soc*., 1962, **84**, 1393.
11 C. H. Chang, R. F. Porter and S. H. Bauer, *J. Mol. Struct. (THEOCHEM)*, 1971, **7**, 89.
12 H. H. Claassen, *J. Chem. Phys*., 1950, **18**, 543.
13 A. R. Ravishankara, S. Solomon, A. A. Turnipseed and R. F. Warren, *Science*, 1993, **259**, 194.
14 D. L. Smith and L. Kevan, *J. Chem. Phys*., 1971, **55**, 2290.
15 C. Q. Jiao, A. Garscadden and P. D. Haaland, *Chem. Phys. Lett*., 1998, **297**, 121.
16 R. A. Morris, A. A. Viggiano, S. T. Arnold and J. F. Paulson, *Int. J. Mass Spectrom. Ion Processes*, 1995, **149/150**, 287.
17 G. K. Jarvis, K. J. Boyle, C. A. Mayhew and R. P. Tuckett, *J. Phys. Chem. A*, 1998, **102**, 3230.
18 K. Hiraoka, T. Mizuno, D. Eguchi, K. Takao and T. Iino, *J. Chem. Phys*., 2002, **116**, 7574.
19 G. K. Jarvis, R. A. Kennedy, C. A. Mayhew and R. P. Tuckett, *Int. J. Mass Spectrom*., 2000, **202**, 323.
20 P. A. Hatherly, D. M. Smith and R. P. Tuckett, *Z. Phys. Chem*., 1996, **195**, 97.
21 D. M. P. Holland, J. B. West, A. A. Macdowell, I. H. Munro and A. G. Beckett, *Nucl. Instrum. Methods Phys. Res., Sect. B*, 1989, **44**, 233.
22 D. Smith and N. G. Adams, *Adv. At. Mol. Phys*., 1988, **24**, 1.
23 D. K. Böhme, *Int. J. Mass Spectrom*., 2000, **200**, 97.
24 V. A. Mikhailov, M. A. Parkes, R. P. Tuckett and C. A. Mayhew, *J. Phys. Chem. A*, 2006, **110**, 5760.
25 M. J. Frisch, G. W. Trucks, H. B. Schlegel, G. E. Scuseria, M. A. Robb, J. R. Cheeseman, J. A. Montgomery, Jr, T. Vreven, K. N. Kudin, J. C. Burant, J. M. Millam, S. S. Iyengar, J. Tomasi, V. Barone, B. Mennucci, M. Cossi, G. Scalmani, N. Rega, G. A. Petersson, H. Nakatsuji, M. Hada, M. Ehara, K. Toyota, R. Fukuda, J. Hasegawa, M. Ishida, T. Nakajima, Y. Honda, O. Kitao, H. Nakai, M. Klene, X. Li, J. E. Knox, H. P. Hratchian, J. B. Cross, V. Bakken, C. Adamo, J. Jaramillo, R. Gomperts, R. E. Stratmann, O. Yazyev, A. J. Austin, R. Cammi, C. Pomelli, J. W. Ochterski, P. Y. Ayala, K. Morokuma, G. A. Voth, P. Salvador, J. J. Dannenberg, V. G. Zakrzewski, S. Dapprich, A. D. Daniels, M. C. Strain, O. Farkas, D. K. Malick, A. D. Rabuck, K. Raghavachari, J. B. Foresman, J. V. Ortiz, Q. Cui, A. G. Baboul, S. Clifford, J. Cioslowski, B. B. Stefanov, G. Liu, A. Liashenko, P. Piskorz, I. Komaromi, R. L. Martin, D. J. Fox, T. Keith, M. A. Al-Laham, C. Y. Peng, A. Nanayakkara, M. Challacombe, P. M. W. Gill, B. Johnson, W. Chen, M. W. Wong, C. Gonzalez, J. A. Pople, *GAUSSIAN 03 (Revision C.02)*, Gaussian, Inc., Wallingford CT, 2004.
26 M. A. Parkes, R. Y. L. Chim, C. A. Mayhew, V. A. Mikhailov and R. P. Tuckett, *Mol. Phys*., 2006, **104**, 263.
27 J. C. Traeger and R. G. McLoughlin, *J. Am. Chem. Soc*., 1981, **103**, 3647.
28 W. Zhou, D. J. Collins, R. Y. L. Chim, D. P. Seccombe and R. P. Tuckett, *Phys. Chem. Chem. Phys*., 2004, **6**, 3081.
29 M. W. Chase, *J. Phys. Chem. Ref. Data*, 1998, monograph no. 9.
30 http://webbook.nist.gov/chemistry.
31 S. G. Lias, J. E. Bartmess, J. F. Lebman, J. L. Holmes, R. D. Levin and W. G. Mallard, *J. Phys. Chem. Ref. Data*, 1988, **17**(supplement no. 1).
32 S. W. Benson and H. E. O'Neal, *Natl. Stand. Ref. Data Ser*., 1970, NBS-21.
33 C. Bauschlicher and A. Ricca, *J. Phys. Chem. A*, 2000, **104**, 4581.
34 G. A. Garcia, P. M. Guyon and I. Powis, *J. Phys. Chem. A*, 2001, **105**, 8296.
35 R. Y. L. Chim, R. A. Kennedy, R. P. Tuckett, W. Zhou, G. K Jarvis, D. J. Collins and P. A. Hatherly, *J. Phys. Chem. A*, 2001, **105**, 8403.
36 T. Su and W. J. Chesnavich, *J. Chem. Phys*., 1982, **76**, 5183.
37 T. Su, *J. Chem. Phys*., 1988, **89**, 5355.
38 P. M. Langevin, *Ann. Chim. Phys*., 1905, **5**, 245.
39 P. K. Bhowmik and T. Su, *J. Chem. Phys*., 1991, **94**, 6444.
40 C. W. Bauschlicher and A. Ricca, *J. Phys. Chem*., 2000, **104**, 9026.
41 T. Shimanouchi, *Tables of Molecular Vibrational, Frequencies consolidated volume 1*, National Bureau of Standards, 1972, p. 1.
42 R. B. Woodward and R. Hoffmann, *The Conservation of Orbital Symmetry*, Verlag Chemie, Weinheim, 1970.
43 G. L. D. Ritchie, private communication.
44 G. L. D. Ritchie and J. N. Watson, *Chem. Phys. Lett*., 2000, **322**, 143.
45 Y. Ikezoe, S. Matsuoka, M. Takebe and A. A. Viggiano, *Gas-phase ion-molecule rate constants through 1986*, Maruzen Company Ltd, Tokyo, 1987.
46 R. Janoschek and M. J. Rossi, *Int. J. Chem. Kinet*., 2004, **36**, 661.
47 R. Janoschek and M. J. Rossi, *Int. J. Chem. Kinet*., 2002, **34**, 550.
48 K. K. S. Lau, K. K. Gleason and B. L. Trout, *J. Chem. Phys*., 2000, **113**, 4103.

